

Phototuning selectively hole and electron transport in optically switchable ambipolar transistors

Wassima Rekab,^{1#} Tim Leydecker,^{1#} Lili Hou,¹ Hu Chen,³ Mindaugas Kirkus,³ Camila Cendra,⁴ Martin Herder,⁵ Stefan Hecht,⁵ Alberto Salleo,⁴ Iain Mc Culloch,^{2,3} Emanuele Orgiu,^{1,6} Paolo Samori^{1*}*

¹ Université de Strasbourg, CNRS, ISIS, 8 allée Gaspard Monge, 67000 Strasbourg, France.

² Department of Chemistry and Centre for Plastic, Imperial College London, Exhibition Road, London, SW7 2AZ, UK

³ King Abdullah University of Science and Technology (KAUST), Kaust Solar Center (KSC), Thuwal, 23955-6900, Saudi Arabia

⁴ Department of Materials Science and Engineering, Stanford University, Stanford, California 94305, USA

⁵ Department of Chemistry & IRIS Adlershof, Humboldt-Universität zu Berlin, Brook-Taylor-Str. 2, 12489 Berlin, Germany.

⁶ Present address: INRS-Centre Énergie Matériaux Télécommunications, 1650 Blv. Lionel-Boulet, J3X 1S2 Varennes, Québec.

These authors equally contributed to this work.

Corresponding authors: E-mail: samori@unistra.fr , emanuele.orgiu@emt.inrs.ca

KEYWORDS: Semiconducting polymers, diarylethenes, organic field-effect transistors, ambipolar transport, photochromic molecules

ABSTRACT:

One of the grand challenges in organic electronics is to develop multicomponent materials wherein each component imparts a different and independently addressable property to the hybrid system. In this way, the combination of the pristine properties of each component is not only preserved but also combined with unprecedented properties emerging from the mutual interaction between the components. Here we show, for the first time, that tri-component materials comprised of an ambipolar diketopyrrolopyrrole-based semiconducting polymer combined with two different photochromic diarylethene molecules possessing ad hoc energy levels can be used to develop organic field-effect transistors, in which the transport of both, holes and electrons, can be photo-modulated. We demonstrate a fully reversible light-switching process, with a light-controlled 100-fold modulation of *p*-type charge transport and a 10-fold modulation of *n*-type charge transport. These findings pave the way for photo-tunable inverters and ultimately for completely re-addressable high-performance circuits comprising optical storage units and ambipolar field-effect transistors.

INTRODUCTION

Organic semiconductors are ideal active components for low-cost, flexible displays and large-area electronics, owing to their relative ease of processing from solution and at room temperature.^[1] Ambipolar organic field-effect transistors (OFETs)^[2] represent an advance towards the development of organic complementary circuits (CMOS)^[3] by incorporating both *p*- and *n*-type transistors. At the same time, blending semiconducting polymers with small molecules enables further tuning of optical and electrical properties, thus creating a powerful strategy to leverage the device performance.^[4] Among the different functional molecules, photochromic molecules are capable of undergoing efficient and reversible photochemical isomerization between (meta)stable states, which exhibit markedly different properties such as light absorption, polarity, and redox behavior.^[5] These molecules have been combined with organic semiconductors in order to control the overall material's properties and thus device performance with an optical input, resulting in light-responsive transistors^[6] and memories.^[7] Photochromic molecules were placed at the semiconductor-insulator interface,^[8] as a self-assembled monolayer on the electrodes,^[9] or blended with organic semiconductors^[10] to control optical and electrical characteristics. Among photochromic molecules, diarylethene derivatives^[11] are very promising building blocks, combining good thermal stability and fatigue resistance.^[12] These diarylethene moieties possess different highest occupied molecular orbital (HOMO) and lowest unoccupied molecular orbital (LUMO) levels, depending on their stronger (closed isomer) or weaker (open isomer) extent of π -conjugation, which can be controlled upon irradiating at different wavelengths.^[13] It was established that the incorporation of diarylethenes (DAEs) into either *p*-type^[14] or *n*-type^[15] semiconductors could ultimately lead to transistors with phototunable charge transport. The

exceptional stability of these photochromic molecules in both open and closed forms could furthermore be exploited for the fabrication of non-volatile photoswitchable multilevel memories.^[16] While phototunable energy levels could be introduced in *n*-type/DAE and *p*-type/DAE blends, the possibility to optically control electrons and holes *simultaneously* in an ambipolar bi-component semiconductor would be highly interesting towards fabricating light-controllable organic-based CMOS-like devices.

Here, we report on the fabrication and characterization of ambipolar transistors whose *n*-type and *p*-type currents can be selectively and reversibly photo-gated upon irradiation at different wavelengths. In particular, we fabricate and characterize three-terminal devices whose active layer is based on simultaneous integration of two different diarylethenes derivatives into a polymer matrix capable of efficiently transporting both holes and electrons.

Ambipolar transistors based on a diketopyrrolopyrrole-thieno[3,2-*b*]thiophene copolymer (DPPT-TT, Fig. 1a) as the active layer were fabricated in a bottom-contact, bottom-gate configuration, on a SiO₂/n⁺⁺-Si substrate. Two diarylethene derivatives highly robust to (optical) switching fatigue^[12], i.e. DAE_tBu (Fig. 1b) and DAE_F (Fig. 1c), were integrated into a matrix of DPPT-TT. DPPT-TT was selected since it has previously been demonstrated^[17] that it can be processed into ambipolar thin films featuring balanced hole and electron mobilities upon thermal annealing at 320 °C for 20 minutes. Given that the DAE derivatives are not stable at such a high temperature, these photochromic molecules were subsequently incorporated into the polymer matrix via temperature assisted permeation at a lower temperature, i.e. 90 °C (Fig. 2a).

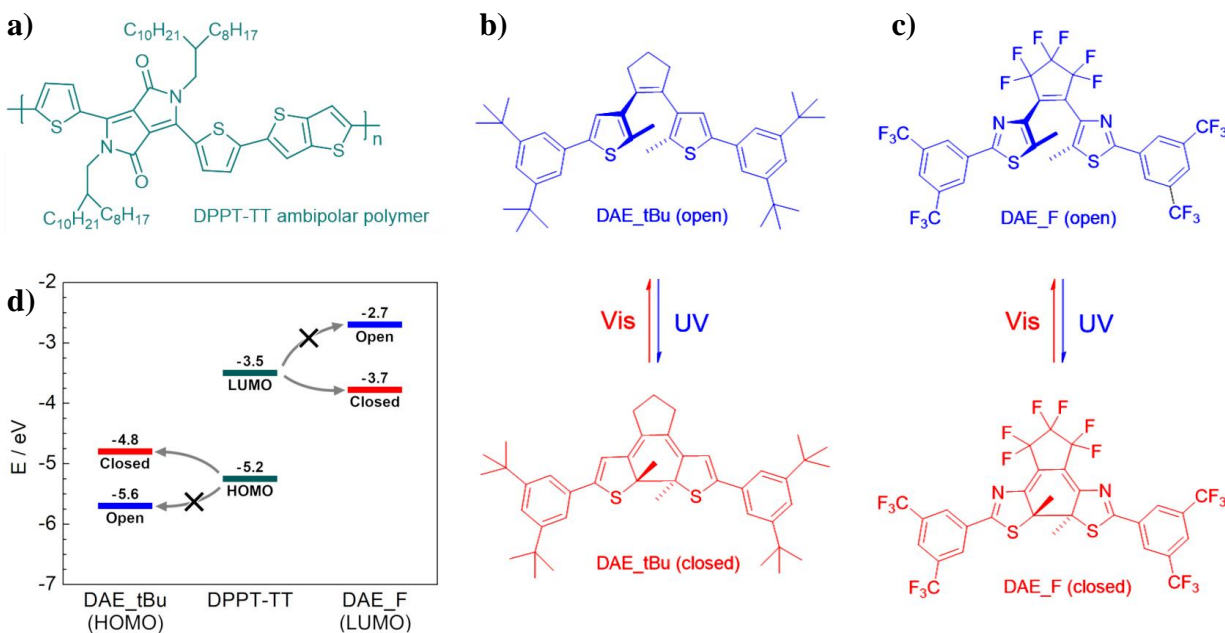


Figure 1. Molecular structures and energy diagrams. Molecular structures of **a)** diketopyrrolopyrrole-thieno[3,2-b]thiophene copolymer (DPPT-TT), **b)** the open and closed form of DAE_tBu and **c)** DAE_F. **d)** Schematic energy diagram representing the HOMO and LUMO levels of DPPT-TT ambipolar polymer and photochromic diarylethenes (DAE_tBu and DAE_F) in their open and closed states (energy levels measured by cyclic voltammetry).^[14b, 18]

Owing to the electronic interactions between the chosen polymer and the DAE molecules, the output (drain) current of the as-fabricated OFET can be photo-tuned.^[6, 19] Depending on their isomeric form, i.e. open or closed switching state, DAEs feature different HOMO and LUMO levels (Fig. 1d). The $\text{HOMO}_{[\text{DAE}_t\text{Bu, closed}]}$ and $\text{LUMO}_{[\text{DAE}_F, \text{closed}]}$ lie at energy values, which are comprised within the DPPT-TT bandgap, and thus act as hole and electron accepting levels, respectively. In both cases, such mechanism results in a device current decrease. Importantly, the $\text{HOMO}_{[\text{DAE}_t\text{Bu, open}]}$ and $\text{LUMO}_{[\text{DAE}_F, \text{open}]}$ levels do not fall within DPPT-TT bandgap, thus no

opposing electronic interactions take place. In other words, hole and electron channels are clearly defined.

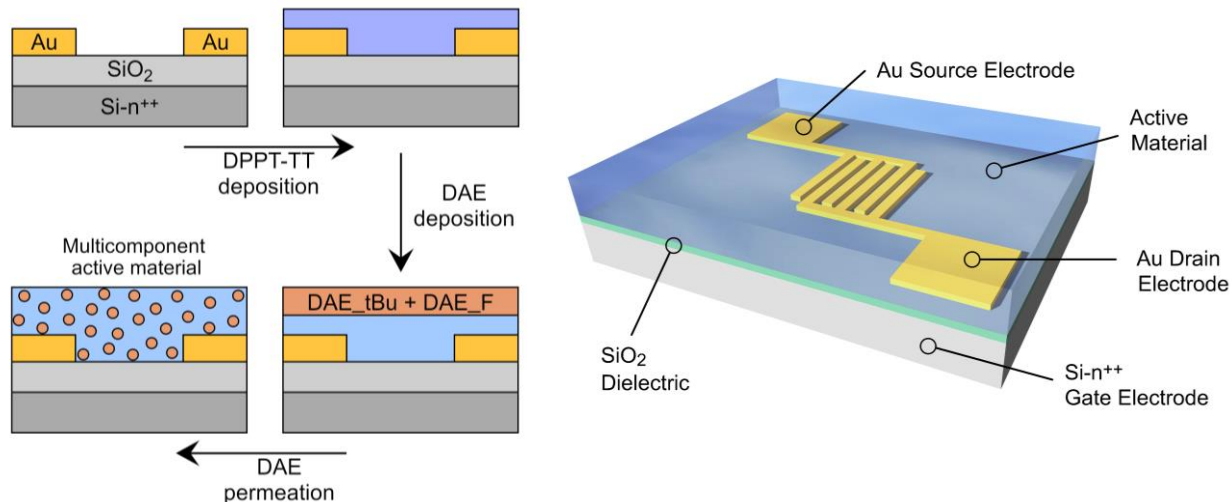


Figure 2. Device fabrication a) Schematic illustration of the preparation steps of OFET device in a bottom-contact bottom-gate geometry based on DPPT-TT polymer as the active layer with diarylethene molecules permeated into its matrix. b) Illustration of the final device.

The ambipolar OFETs were characterized in the dark before and after adding DAEs into the polymer layer, to investigate the effect of DAEs insertion on the electron and hole mobilities. The electrical characteristics of OFET devices were measured in order to extract hole and electron field-effect mobility (μ_h and μ_e), threshold voltage (V_{th}) and I_{on}/I_{off} . Device transfer curves recorded prior DAE deposition (Fig. S2 in the Supporting Information) displayed typical ambipolar characteristics with good hole transport characteristics ($\mu_h \sim 0.5 \text{ cm}^2\text{V}^{-1}\text{s}^{-1}$ and $I_{on}/I_{off} \sim 10^7$) but lower electron-transport characteristics ($\mu_e \sim 0.012 \text{ cm}^2\text{V}^{-1}\text{s}^{-1}$, $I_{on}/I_{off} \sim 10^5$). Mobilities could be further improved through octadecyltrichlorosilane (OTS) treatment of the dielectric support, reaching $\mu_h \sim 0.6 \text{ cm}^2\text{V}^{-1}\text{s}^{-1}$ and $\mu_e \sim 0.017 \text{ cm}^2\text{V}^{-1}\text{s}^{-1}$, respectively. These mobility values

were comparable with previous reports^[20] on bottom-gate, bottom-contact devices. Higher electron and hole mobilities ($\mu_h \sim 1.36 \text{ cm}^2\text{V}^{-1}\text{s}^{-1}$ and $\mu_e \sim 1.56 \text{ cm}^2\text{V}^{-1}\text{s}^{-1}$) of the same polymer have been reported for top-gate bottom-contact devices.^[17] To compare these performances, OFETs in top-gate bottom-contact configuration were fabricated (Fig. S1). The transfer characteristics for hole and electron transport as well as the electrical parameters are presented in the Supporting Information (Fig. S2, Table S1). These top-gate devices exhibited improved mobilities ($\mu_e \sim 0.11 \text{ cm}^2\text{V}^{-1}\text{s}^{-1}$, $I_{\text{on}}/I_{\text{off}} \sim 10^5$, and $\mu_h \sim 4.2 \text{ cm}^2\text{V}^{-1}\text{s}^{-1}$, $I_{\text{on}}/I_{\text{off}} \sim 10^6$). However, since in a top-gate architecture most of the light during *in-situ* irradiation would be absorbed by the gate metal and the insulating polymer, we focused our attention on DPPT-TT-DAE transistors in bottom-gate bottom-contact configuration.

Bi- and three-component devices based on DPPT-TT with 10 wt% of one or two DAE molecules (DAE_tBu and DAE_F) as the active layer were fabricated. Comparison of the electrical performances of OFETs before and after DAEs deposition (Fig. S3 in the Supporting Information) revealed that DAEs incorporation resulted in a small decrease in mobility (Table S2 in the Supporting Information). The morphology of pristine polymer and DAE-containing films was studied by atomic force microscopy (AFM) by imaging single, bi-and three- component devices (Fig. S4 in the Supporting Information). The AFM analysis revealed unaltered film morphology on the micrometer scale upon permeation of DAEs through the polymer film, characterized by tightly packed lamellar structures. The root mean square roughness (R_{RMS}) of the different films was determined in an area of $5 \times 5 \text{ }\mu\text{m}^2$ (Table S3 in the Supporting Information) and displays only slightly higher values in bi-and three-component based devices ($R_{\text{RMS}} = 1.47\text{-}1.79 \text{ nm}$) when compared to pristine DPPT-TT polymer films ($R_{\text{RMS}} = 1.14 \text{ nm}$). To cast further light onto the effect of DAE incorporation on the crystalline structure of the polymer, grazing incident x-ray

diffraction (GIXD) measurements were performed (Fig. S9 and Table S4 in the Supporting Information). These measurements revealed that the permeation of DAEs into the polymer matrix did not result in any major disruption of semiconductor molecular packing. Such result is in accordance with previous reports of diarylethenes incorporated in a polymer matrix.^[14b]

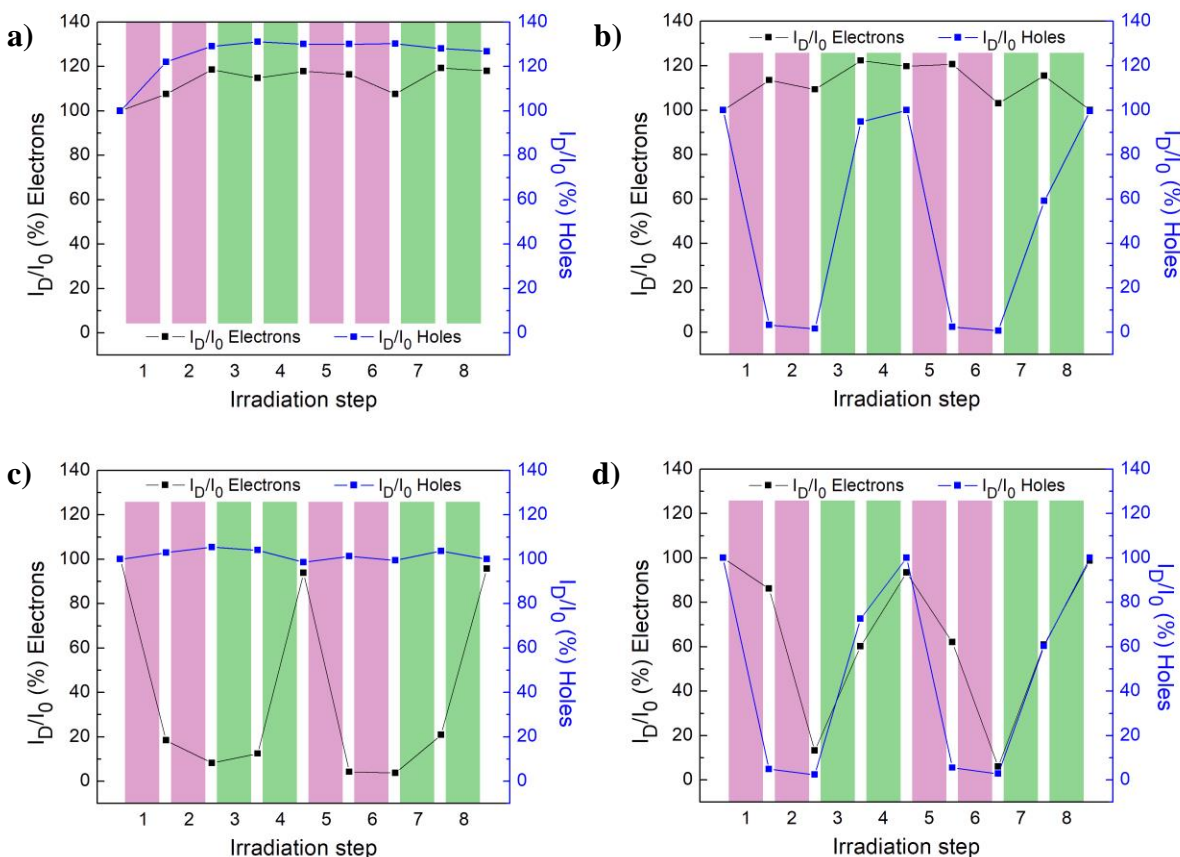


Figure 3. OFET characteristics under ultraviolet and visible light irradiation. I_D/I_0 of OFET devices based on **a)** pristine DPPT-TT, **b)** DPPT-TT with DAE_tBu (10 wt %), **c)** DPPT-TT with DAE_F (10 wt %) and **d)** DPPT-TT with both 10 wt % of DAE_tBu and 10 wt % of DAE_F. Violet and green shaded areas correspond to the irradiation with light at wavelengths of 365 nm and 546 nm, respectively. The irradiation is performed from above the devices. All irradiation steps power and duration are detailed in section 1 of the Supporting Information.

The effect of light irradiation wavelength on the drain current was investigated by exposing bi- and tri-component OFETs to ultraviolet ($\lambda = 365$ nm) and green ($\lambda = 546$ nm) LEDs under nitrogen atmosphere. Light irradiation was found to induce a marked modulation of hole and electron drain current as shown in Fig. 3 for devices of DPPT-TT with permeated DAE_tBu (Fig. 3b), and with permeated DAE_F (Fig. 3c). Remarkably, it was possible to induce both hole and electron drain current modulation in the three-component devices (Fig. 3d). As expected, devices based on the pristine polymer on DPPT-TT did not exhibit any change in current upon irradiation (Fig. 3a).

In the bi-component devices based on the polymer with inserted DAE_tBu molecules (Fig. 3b), the hole drain current decreased by two orders of magnitude upon UV illumination. Upon irradiation with visible light, the current recovered to 98% of the initial value, while the electron current remained constant upon irradiation in the UV and in the visible. In DPPT-TT/DAE_F OFETs, the electron current was modulated upon UV and visible illumination by a factor of 10, while the hole current remained stable. Upon UV light irradiation, the drain current extracted from three-component devices exhibited a decrease of 92% and 85% for holes and electrons, respectively (Fig. 3d). After visible light irradiation (two steps of 5 minutes), the drain current of the electron and hole increased and completely recovered. The ability to optically switch the output current of our OFETs indicates that DAE molecules efficiently diffuse through the polymer matrix and reach the semiconductor-dielectric interface.

These results confirm the light-switching process, which is completely reversible and selective for both hole and electron charge transport. Furthermore, the large light-induced current modulation was maintained, even after the devices were stored for several months inside the glove

box, indicating that small diarylethene molecules non-covalently bound into polymer matrices can be used in robust optical memories.

The retention of the photo-switching ability of DAEs diffused into DPPT-TT matrix was further investigated by UV/visible absorption spectroscopy. UV and visible light irradiation on neat DAE_tBu and DAE_F in solution (Fig. S5 in the Supporting Information) and in films (Fig. S8 in the Supporting Information), result in the appearance and disappearance of the absorption band between 400-600 nm. After diffusion into the DPPT-TT film, UV irradiation at $\lambda = 312$ nm led to an increase in absorption in the $\lambda = 400$ -600 nm region for both DAE_tBu (Fig. S6a in the Supporting Information), and DAE_F films (Fig. S7a in the Supporting Information), corresponding to the formation of the closed-ring isomer.^[21] Subsequent irradiation of the films with visible light ($\lambda = 530$ nm), to switch the molecules back to the open-ring isomer, resulted in spectral recovery of the initial states (Fig. S6b for DAE_tBu, Fig. S7b for DAE_F in the Supporting Information), confirming the reversible nature of DAE photo-switching in the DPPT-TT films.

The photochemical quantum yield (QY) for the photoisomerization from the ring-closed form to the open-ring isomer of DAEs in the polymer matrix was determined as $\Phi = 0.003$ for DAE_tBu and $\Phi = 0.02$ for DAE_F. The lower QYs, compared to those measured in solution ($\Phi = 0.009$ for DAE_tBu and $\Phi = 0.039$ for DAE_F)^[12, 14a], are expected as the polymer matrix hinders the change in the molecular configuration. Nevertheless, these QYs remain high enough to enable an efficient photoswitching of the output current in the OFETs.

In summary, photo-modulation of the output current in ambipolar field-effect transistors was achieved through the fabrication of multicomponent devices based on an active layer of DPPT-TT with permeated DAEs. The light-switching process in films was completely reversible and selective using DAE_tBu and/or DAE_F as photochromic molecules. The drain current of the

OFETs was reversibly modulated by alternating ultraviolet and visible light irradiation, with a 100- and 10-fold modulation of charge transport in the *p*- and *n*-channel, respectively. Most importantly, extreme versatility was demonstrated as one and the same polymer, DPPT-TT, was used and processed in the identical fashion to produce three types of photoswitchable OFETs (*p*-type, *n*-type and ambipolar) upon selected diarylethene diffusion. This finding is of paramount practical relevance, as it demonstrates that large-area electronics could be easily produced from a homogeneous high-performance ambipolar film, and selectively modified to obtain ambipolar, *p*-type conducting, *n*-type conducting as well as insulating regions through careful selection, deposition, and operation of photoswitchable moieties. Since the diffusion method demonstrated no adverse effect on the charge transport (both for *p*-type and *n*-type carriers), this approach can be employed without loss of performance. Furthermore, the results highlighted in this article pave the way for photoswitchable ambipolar transistors with separate hole and electron charge transport modulation, leading to circuits that could be completely redesigned by simple light-based writing for a new generation of evolutive electronics.

REFERENCES

- [1] K. J. Baeg, M. Caironi, Y. Y. Noh, *Adv. Mater.* **2013**, 25, 4210.
- [2] a) Y. Zhao, Y. L. Guo, Y. Q. Liu, *Adv. Mater.* **2013**, 25, 5372; b) J. Zaumseil, H. Sirringhaus, *Chem. Rev.* **2007**, 107, 1296; c) E. C. P. Smits, T. D. Anthopoulos, S. Setayesh, E. van Veenendaal, R. Coehoorn, P. W. M. Blom, B. de Boer, D. M. de Leeuw, *Phys. Rev. B* **2006**, 73.
- [3] a) T. B. Singh, P. Senkarabacak, N. S. Sariciftci, A. Tanda, C. Lackner, R. Hagelauer, G. Horowitz, *Appl. Phys. Lett.* **2006**, 89; b) A. Petritz, A. Fian, E. D. Glowacki, N. S. Sariciftci, B. Stadlober, M. Irimia-Vladu, *Phys. Status Solidi Rapid Res. Lett.* **2015**, 9, 358.
- [4] a) E. Orgiu, A. M. Masillamani, J. O. Vogel, E. Treossi, A. Kiersnowski, M. Kastler, W. Pisula, F. Dotz, V. Palermo, P. Samori, *Chem. Commun.* **2012**, 48, 1562; b) R. Hamilton, J. Smith, S. Ogier, M. Heeney, J. E. Anthony, I. McCulloch, J. Veres, D. D. C. Bradley, T. D. Anthopoulos, *Adv. Mater.* **2009**, 21, 1166; c) M. Kang, H. Hwang, W. T. Park, D.

- Khim, J. S. Yeo, Y. Kim, Y. J. Kim, Y. Y. Noh, D. Y. Kim, *ACS Appl. Mater. Inter.* **2017**, 9, 2686.
- [5] a) V. A. Pichko, B. Y. Simkin, V. I. Minkin, *J. Org. Chem.* **1992**, 57, 7087; b) M. Irie, T. Fulcaminato, K. Matsuda, S. Kobatake, *Chem. Rev.* **2014**, 114, 12174.
- [6] F. L. E. Jakobsson, P. Marsal, S. Braun, M. Fahlman, M. Berggren, J. Cornil, X. Crispin, *J. Phys. Chem. C* **2009**, 113, 18396.
- [7] a) L. A. Frolova, P. A. Troshin, D. K. Susarova, A. V. Kulikov, N. A. Sanina, S. M. Aldoshin, *Chem. Commun.* **2015**, 51, 6130; b) T. Tsujioka, H. Kondo, *Appl. Phys. Lett.* **2003**, 83, 937.
- [8] R. C. Shallcross, P. O. Korner, E. Maibach, A. Kohnen, K. Meerholz, *Adv. Mater.* **2013**, 25, 4807.
- [9] T. Mosciatti, M. G. del Rosso, M. Herder, J. Frisch, N. Koch, S. Hecht, E. Orgiu, P. Samorì, *Adv. Mater.* **2016**, 28, 6606.
- [10] R. Hayakawa, K. Higashiguchi, K. Matsuda, T. Chikyow, Y. Wakayama, *ACS Appl. Mater. Inter.* **2013**, 5, 3625.
- [11] M. Irie, *Photoch. Photobio. Sci.* **2010**, 9, 1535.
- [12] M. Herder, B. M. Schmidt, L. Grubert, M. Patzel, J. Schwarz, S. Hecht, *J. Am. Chem. Soc.* **2015**, 137, 2738.
- [13] a) A. Perrier, F. Maurel, D. Jacquemin, *J. Phys. Chem. C* **2011**, 115, 9193; b) S. Nakamura, S. Yokojima, K. Uchida, T. Tsujioka, *J. Photoch. Photobio. C* **2011**, 12, 138.
- [14] a) M. El Gemayel, K. Borjesson, M. Herder, D. T. Duong, J. A. Hutchison, C. Ruzie, G. Schweicher, A. Salleo, Y. Geerts, S. Hecht, E. Orgiu, P. Samorì, *Nat. Commun.* **2015**, 6, 6330; b) E. Orgiu, N. Crivillers, M. Herder, L. Grubert, M. Patzel, J. Frisch, E. Pavlica, D. T. Duong, G. Bratina, A. Salleo, N. Koch, S. Hecht, P. Samorì, *Nat. Chem.* **2012**, 4, 675.
- [15] K. Borjesson, M. Herder, L. Grubert, D. T. Duong, A. Salleo, S. Hecht, E. Orgiu, P. Samorì, *J. Mater. Chem. C* **2015**, 3, 4156.
- [16] T. Leydecker, M. Herder, E. Pavlica, G. Bratina, S. Hecht, E. Orgiu, P. Samorì, *Nat. Nanotechnol.* **2016**, 11, 769.
- [17] Z. Y. Chen, M. J. Lee, R. S. Ashraf, Y. Gu, S. Albert-Seifried, M. M. Nielsen, B. Schroeder, T. D. Anthopoulos, M. Heeney, I. McCulloch, H. Sirringhaus, *Adv. Mater.* **2012**, 24, 647.
- [18] a) K. Borjesson, M. Herder, L. Grubert, D. T. Duong, A. Salleo, S. Hecht, E. Orgiu, P. Samorì, *J. Mater. Chem. C* **2015**, 3, 4156; b) J. Li, Y. Zhao, H. S. Tan, Y. L. Guo, C. A. Di, G. Yu, Y. Q. Liu, M. Lin, S. H. Lim, Y. H. Zhou, H. B. Su, B. S. Ong, *Sci. Rep.* **2012**, 2.
- [19] T. Koshido, T. Kawai, K. Yoshino, *Synth. Met.* **1995**, 73, 257.
- [20] X. R. Zhang, L. J. Richter, D. M. DeLongchamp, R. J. Kline, M. R. Hammond, I. McCulloch, M. Heeney, R. S. Ashraf, J. N. Smith, T. D. Anthopoulos, B. Schroeder, Y. H. Geerts, D. A. Fischer, M. F. Toney, *J. Am. Chem. Soc.* **2011**, 133, 15073.
- [21] a) M. Irie, *Chem. Rev.* **2000**, 100, 1685; b) K. Matsuda, M. Irie, *J. Photoch. Photobio. C* **2004**, 5, 169.

ACKNOWLEDGMENT

We acknowledge funding from the European Commission through the Marie Skłodowska-Curie ITN project iSwitch (GA-642196), the ERC projects SUPRAFUNCTION (GA-257305) and LIGHT4FUNCTION (GA-308117), the Agence Nationale de la Recherche through the Labex project CSC (ANR-10-LABX-0026 CSC) within the Investissement d’Avenir program (ANR-10-120 IDEX-0002-02), the Région Grand Est project HARWEST and the International Center for Frontier Research in Chemistry (icFRC) as well as the German Research Foundation (via SFB 765 and SFB 951). Use of the Stanford Synchrotron Radiation Lightsource, SLAC National Accelerator Laboratory, is supported by the U.S. Department of Energy, Office of Science, Office of Basic Energy Sciences under Contract No. DE-AC02-76SF00515

Methods

Experimental details are reported in the Supporting Information.

ASSOCIATED CONTENT

Supporting Information

Additional results, including electrical characterization obtained from the extraction of the major device parameters, absorption spectra, and Atomic Force Microscopy, as well as grazing incident x-ray diffraction (GIXD) measurements were performed in order to provide a complete morphological and energetical overview of this three-component system.

Table of contents

